

The proper motion of PSR J1550–5418 measured with VLBI: a second magnetar velocity measurement

A. T. Deller¹, F. Camilo², J. E. Reynolds³, and J. P. Halpern²

ABSTRACT

The formation mechanism of neutron stars with extremely large magnetic field strengths (magnetars) remains unclear. Some formation scenarios predict that magnetars should be born with extremely high space velocities, $> 1000 \text{ km s}^{-1}$. Using the Long Baseline Array in Australia, we have measured the proper motion of the intermittently radio-bright magnetar PSR J1550–5418 (1E 1547.0–5408): $\mu = 9.2 \pm 0.6 \text{ mas yr}^{-1}$. For a likely distance of $6 \pm 2 \text{ kpc}$, the implied transverse velocity is $280^{+130}_{-120} \text{ km s}^{-1}$ after correcting for Galactic rotation. Along with the $\approx 200 \text{ km s}^{-1}$ transverse velocity measured for the magnetar XTE J1810–197, this result suggests that formation pathways producing large magnetic fields do not require very large birth kicks.

Subject headings: astrometry — pulsars: individual (PSR J1550–5418, 1E 1547.0–5408) — stars: neutron

1. Introduction

Magnetars, originally identified via their bright and variable high-energy emission, are neutron stars largely powered by the decay of ultra-strong magnetic fields (Duncan & Thompson 1992). Known examples of magnetars¹ – both anomalous X-ray pulsars (AXPs) and soft gamma-ray repeaters (SGRs) – are young, but rotate slowly because their strong dipole fields ($B_s \sim 10^{14-15} \text{ G}$) have spun them down quickly. Duncan & Thompson (1992) and Thompson & Duncan (1993) suggested that such large fields can only be created through dynamo action in proto-neutron stars with $\sim 1 \text{ ms}$ spin periods, which is shorter than the

¹ASTRON, P.O. Box 2, 7990 AA Dwingeloo, The Netherlands

²Columbia Astrophysics Laboratory, Columbia University, 550 West 120th Street, New York, NY 10027, USA

³Australia Telescope National Facility, CSIRO, Epping, NSW 1710, Australia

¹<http://www.physics.mcgill.ca/~pulsar/magnetar/main.html>.

convective overturn time. Searches for evidence of such fast initial rotation via its enhanced contribution, up to 10^{52} erg, to the explosion energy of the supernova remnants (SNRs) hosting magnetars, have generally come up negative (Vink & Kuiper 2006; Halpern & Gotthelf 2010). On the other hand, it is possible that the diffusion of such rotational energy through the envelope of a supernova can explain some of the most luminous SNe light curves that have been observed in recent years (Kasen & Bildstein 2010). The birth of a millisecond magnetar is also considered a possible channel for gamma-ray bursts.

A possible consequence of the large internal magnetic fields ($B \geq 10^{15}$ G) or fast initial rotation ($P \leq 1$ ms) of magnetars is a very high kick velocity. Processes that are ineffective in ordinary neutron stars, but may produce $v > 1000 \text{ km s}^{-1}$ recoils in magnetars, include anisotropic mass loss in a wind or jet, the electromagnetic rocket effect, and anisotropic neutrino emission (Duncan & Thompson 1992; Thompson & Duncan 1993). On the other hand, the central location of some magnetars within SNRs has led to the inference that as a class their velocity is $< 500 \text{ km s}^{-1}$ (Gaensler et al. 2001), closer to that of the population of ordinary pulsars. The superposition of SGRs on massive star clusters or giant molecular clouds (Corbel & Eikenberry 2004) that are considered their likely birth places also offers circumstantial evidence that their velocities are unremarkable.

Attempts to actually measure velocities via X-ray or infrared imaging remain unfilled, and only the first radio-detected magnetar, XTE J1810–197, has a reported proper motion. Using VLBA observations, Helfand et al. (2007) obtained a transverse velocity of $\approx 200 \text{ km s}^{-1}$ for XTE J1810–197, slightly below the average for young neutron stars. Although the unknown radial component of velocity makes it impossible to draw firm conclusions, this result is not supportive of theories of magnetar formation mechanisms that require a high initial velocity. However, more measurements are required in order to actually measure the initial velocity distribution of this exotic class of neutron stars.

The discovery of a second radio-emitting magnetar, PSR J1550–5418 (Camilo et al. 2007), provided the opportunity for a second proper motion measurement. Here we present Long Baseline Array observations and the resulting proper motion for this 2 s pulsar (also known as 1E 1547.0–5408). Our VLBI observations and results are presented in Sections 2 and 3, and the implications for the birth velocity of PSR J1550–5418 and magnetars in general are discussed in Section 4.

2. VLBI observations

We observed PSR J1550–5418 five times over a period of 2.5 years using Australia’s Long Baseline Array (LBA). The LBA consists of six antennas: the Australia Telescope Compact Array (ATCA), Parkes, Mopra and Tidbinbilla antennas operated by CSIRO Astronomy and Space Sciences, and the Hobart and Ceduna antennas operated by the University of Tasmania. The first observation, obtained using a target of opportunity trigger in 2007 August, was made at 2.3 GHz, and revealed that PSR J1550–5418 suffers from severe scatter broadening due to the intervening ionized interstellar medium (already measured in the time domain by Camilo et al. 2007). PSR J1550–5418 was detected on the shortest baselines only, and the scatter broadening was estimated to be approximately 80 milliarcseconds (mas) at 2.3 GHz. This scatter-broadening exceeds the prediction of the NE2001 model (Cordes & Lazio 2002) for the location of PSR J1550–5418 by a factor of 5. Accordingly, the remaining observations were made at 8.4 GHz, where the effects of scatter-broadening are much less severe and the astrometric precision much higher.

Observing setups varied between epochs due to resource constraints and equipment upgrades, with observation durations between 5 and 12 hours, and total bandwidths of 32 MHz or 64 MHz (dual polarization). Table 1 summarizes the 8.4 GHz observations, which were used for the astrometric results detailed below.

At the commencement of observations, the sparse calibrator grid in the southern skies meant that no known phase reference sources were available within 6° of PSR J1550–5418. Instead, the observations were phase referenced to the bright and compact radio source J1515–5559 (~ 1 Jy at 8 GHz). J1515–5559 was identified as a probable calibrator based on lower-resolution data and confirmed as such in the first astrometric epoch. However, its relatively large angular separation from PSR J1550–5418, 5.3° , means that the quality of phase referencing is much poorer than with other equivalent LBA observations at 8.4 GHz

Table 1. Summary of astrometric observations

Observation date (yyymmdd/MJD)	Participating telescopes ^a	Observing bands ^b (MHz, dual polarization)	Duration (hours)	Detection S/N
071111/54415	AT, CD, HO, MP, PA	8409–8425,8425–8441	5	6
080327/54552	AT, CD, HO, MP, PA	8409–8425,8425–8441,[8441–8457,8457–8473]	12	11
090226/54888	AT, CD, HO, MP, PA	8409–8425,8425–8441,[8441–8457,8457–8473]	10	20
091211/55176	AT, CD, HO, MP, PA, TI	8409–8425,8425–8441,[8441–8457,8457–8473]	8	9

^aAT = Australia Telescope Compact Array, CD = Ceduna, HO = Hobart, MP = Mopra, PA = Parkes, TI = Tidbinbilla.

^bAdditional observing bands listed in square brackets were only present at AT, MP, PA.

(e.g., Deller et al. 2008). A 5 minute target/calibrator cycle was employed, with 2 minute calibrator scans and 3 minute target scans.

After the first epoch, scans to check phase referencing were included on other known calibrator sources within 6° of J1515–5559, and the results used to refine its position. As the position for the calibrator source J1515–5559 was refined in successive observations, different positions were used in correlation at each epoch, but in the final analysis all epochs were corrected to the more accurate position ultimately available in the rfc_2011d VLBI source catalog², (J2000.0) R.A.= $15^h15^m12^s.67312$, decl.= $-55^\circ59'32''.8361$, with errors of 5.4 mas in R.A. and 2.0 mas in decl. This position was derived through observations in the LBA Calibrator Survey, a dedicated southern hemisphere campaign for absolute astrometry (Petrov et al. 2011).

The data were correlated with the DiFX software correlator (Deller et al. 2007), using matched filtering (gating) on pulse profiles. Pulsar ephemerides were supplied at each epoch from accompanying timing observations done with the Parkes telescope, and were used to set gates of widths that ranged between 7.5% and 20% of the pulse period. The applied gate width depended on the (varying) pulse profile at each epoch and the uncertainty in the pulse phase prediction caused by unstable rotation. Due to the relatively high observing frequency of 8.4 GHz, no ionospheric correction was applied after correlation. During some of the observations, the pulsar flux density varied significantly on timescales of hours (these variations are intrinsic to the magnetar; see Camilo et al. 2007, 2008). The amplitudes were flattened (and the data reweighted accordingly) using a ParselTongue script (Kettenis et al. 2006) described in Deller et al. (2009b). Correction of the amplitudes in this manner minimizes the flux scattered away from the true pulsar position and maximizes the significance of the final detection, at the expense of an elongated beam shape due to the time-variable weighting. After imaging using natural weighting, the AIPS task JMFIT was used to estimate positions and errors. The brightness of PSR J1550–5418 varied considerably between epochs, but it was detected in all epochs with a significance ranging from 6σ to 20σ (Table 1), leading to positional fits with a nominal accuracy of $\approx 0.2 - 0.6$ mas.

At 8.4 GHz, the deconvolved, scatter-broadened angular diameter of PSR J1550–5418 was found to be ≈ 6.5 mas. In the four astrometric epochs, fits to the semi-major axis ranged between 5.5 and 8 mas. This angular broadening leaves very little flux on baselines with length $\gtrsim 1000$ km, meaning these baselines contribute very little to the position fit. Consequently, the longest LBA baselines (to Hobart and Ceduna) contributed relatively little to the astrometric accuracy in this project.

²<http://astrogeo.org/vlbi/solutions/rfc2011d/>

3. Astrometric results

Due to the large angular separation between the target and the calibrator, the astrometric errors are dominated not by the signal-to-noise ratio but by systematic contributions. The predominant systematic effects are introduced by the calibrator position uncertainty (~ 5 mas), the station position uncertainties (several centimeters) and the unmodeled atmosphere (delay equivalent to a path length of several centimeters). Both simulations (Pradel et al. 2006) and extrapolation from past results with the LBA (Deller et al. 2008) suggest that under these conditions, the systematic contribution to astrometric error should be of order 1 mas.

For the astrometric fit, the magnetar parallax was fixed at 0.11 mas, corresponding to a distance of 9 kpc (Camilo et al. 2007). Varying the distance over a wide range of values, from 2 kpc to infinity, made an insignificant ($\sim 0.1 \sigma$) change to the proper motion fit. Without the addition of any systematic error estimate, the reduced χ^2 of the fit was 8.0, indicating that as expected the formal errors in fitted position considerably overestimate the astrometric accuracy. The addition of 1.2 mas (R.A.) and 0.6 mas (decl.) errors in quadrature was sufficient to obtain a reduced χ^2 of 1.0. The optimal values for the systematic error (minimizing the squared sum of the R.A. and decl. components) were found via iterative minimization, following the technique used by Deller et al. (2009a). The result of the final fit is shown in Table 2. The absolute positional accuracy of the reference position for PSR J1550–5418 is dominated by the uncertainty in the absolute calibrator position. The observing history of the calibrator source is not long enough to determine if it exhibits time-variable apparent position changes (which would corrupt the target proper motion), but in this case the influence of such effects can be neglected, since the magnitude of such changes are typically $< 0.1 \text{ mas yr}^{-1}$ (e.g., MacMillan & Ma 2007).

Figure 1 shows the positional measurements and fitted motion for PSR J1550–5418. The accuracy is considerably better in decl. than in R.A. due to the predominantly north-south

Table 2. VLBI results for PSR J1550–5418

Parameter	Fitted value and error
R.A. (J2000) ^a	$15^{\text{h}}50^{\text{m}}54.^{\text{s}}12386 \pm 0.^{\text{s}}00005 \pm 0.^{\text{s}}00064$
Decl. (J2000) ^a	$-54^{\circ}18'24.''1141 \pm 0.''0003 \pm 0.''0020$
Epoch of position (MJD)	54795.0
Proper motion in R.A., $\mu_{\alpha} \cos \delta$	$4.8 \pm 0.5 \text{ mas yr}^{-1}$
Proper motion in Decl., μ_{δ}	$-7.9 \pm 0.3 \text{ mas yr}^{-1}$
Total proper motion, μ	$9.2 \pm 0.6 \text{ mas yr}^{-1}$

Note. — All errors listed are 1σ confidence level intervals.

^aCelestial coordinates are given \pm fit errors \pm calibrator position errors.

arrangement of antennas in the LBA.

4. Velocity of PSR J1550–5418 and of magnetars

Our results provide a secure measurement of the proper motion of PSR J1550–5418, but converting this to a transverse velocity requires an estimate of the magnetar’s distance. The free electron column density obtained from the measured dispersion of the radio pulses, along with the electron density model of Cordes & Lazio (2002), suggests that PSR J1550–5418 is located at $d = 9$ kpc (Camilo et al. 2007). The uncertainty on this estimate is unknown, but could approach 50%. An entirely different method relies on modeling three dust-scattered X-ray rings observed following a huge outburst of the magnetar that took place in 2009 January (one month before the third LBA epoch listed in Table 1). Using the scattered X-rays, Tiengo et al. (2010) obtain a best-fit distance of 4 kpc, with anything in the range 4–8 kpc plausible.

We therefore consider that a reasonable distance estimate for PSR J1550–5418 is $d = 6 \pm 2$ kpc. Along with our measured proper motion of $\mu = 9.2 \pm 0.6$ mas yr^{−1} (Table 2), the implied transverse velocity is $v_{\perp} = 260 \pm 90$ km s^{−1}. Correction for peculiar solar motion and Galactic rotation using a flat rotation curve and the current IAU recommended rotation constants ($R_0 = 8.5$ kpc, $\Theta_0 = 220$ km s^{−1}) adjusts this slightly to 280^{+130}_{-120} km s^{−1}, typical for the general population of ordinary pulsars (e.g., Hobbs et al. 2005). This velocity is also comparable to that obtained for the magnetar XTE J1810–197 ($v_{\perp} = 212 \pm 35$ km s^{−1} for $d = 3.5 \pm 0.5$ kpc; Helfand et al. 2007). The small angular velocity of PSR J1550–5418 also implies that an association between the pulsar and the possible SNR shell G327.24–0.13 that apparently surrounds it (Gelfand & Gaensler 2007) remains plausible (see Camilo et al. 2007). Since the characteristic age of the pulsar is ≤ 1400 yr (Camilo et al. 2008), the pulsar could have moved at most $\sim 13''$ since its birth. This is consistent with its location near the centre of the apparent SNR, which has a diameter of $4'$.

With these two proper motions in hand, it is already very unlikely that magnetars as a class have exceptionally high space velocities. For example, if we assume that all magnetars have $v = 1000$ km s^{−1}, then the probability that one will be observed with $v_{\perp} \leq 212$ km s^{−1} is 0.023, while the probability that $v_{\perp} \leq 280$ km s^{−1} is 0.04. Jointly, the probability of both observations is 9×10^{-4} under this assumption. If all magnetars have $v = 500$ km s^{−1}, then the corresponding individual probabilities become 0.094 and 0.171, with 0.016 for the joint probability. We therefore consider $v < 500$ km s^{−1} as a reasonable ($\approx 2.2\sigma$) upper limit on the typical magnetar velocity. Additional measurements or constraints on magnetar proper motions would clearly be desirable to further constrain their distribution of space velocities.

Unfortunately, X-ray observations with *Chandra* have yielded only upper limits that are not very restrictive. Kaplan et al. (2009) find for 1E 2259+586 $\mu < 65 \text{ mas yr}^{-1}$, $v_{\perp} < 930 \text{ km s}^{-1}$ assuming $d = 3 \text{ kpc}$, which is not as small a limit as has already been inferred from the pulsar’s central location in its host SNR CTB 109. For SGR 1900+14, Kaplan et al. (2009) find $\mu < 54 \text{ mas yr}^{-1}$, $v_{\perp} < 1300 \text{ km s}^{-1}$ assuming $d = 5 \text{ kpc}$ (see also De Luca et al. 2009). This result is not constraining if an association of SGR 1900+14 with a young star cluster at $d = 12.5 \text{ kpc}$ is accepted (Vrba et al. 2000; Davies et al. 2009), since SGR 1900+14 remains within $15''$ of the center of the cluster. Similarly, the apparent association of SGR 1806–20 with a cluster of giant massive stars (Fuchs et al. 1999) requires that magnetar to have a small velocity.

The only other known radio-emitting magnetar, PSR J1622–4950 (Levin et al. 2010), is an attractive target for the LBA. But in the meantime, our LBA measurement of the proper motion of PSR J1550–5418 confirms that extremely high velocities need not result as a consequence of the formation of magnetars, and suggests that the velocity distribution of magnetars may not differ significantly from that of ordinary, rotation-powered neutron stars.

The Long Baseline Array and the Parkes Observatory are part of the Australia Telescope, which is funded by the Commonwealth of Australia for operation as a National Facility managed by CSIRO.

REFERENCES

- Camilo, F., Ransom, S. M., Halpern, J. P., & Reynolds, J. 2007, *ApJ*, 666, L93
- Camilo, F., Reynolds, J., Johnston, S., Halpern, J. P., & Ransom, S. M. 2008, *ApJ*, 679, 681
- Corbel, S. & Eikenberry, S. S. 2004, *A&A*, 419, 191
- Cordes, J. M., & Lazio, T. J. W. 2002, *ArXiv e-prints*, 0207156
- Davies, B., Figer, D. F., Kudritzki, R.-P., Trombly, C., Kouveliotou, C., & Wachter, S. 2009, *ApJ*, 707, 844
- Deller, A. T., Tingay, S. J., Bailes, M., & Reynolds, J. E. 2009a, *ApJ*, 701, 1243
- Deller, A. T., Tingay, S. J., Bailes, M., & West, C. 2007, *PASP*, 119, 318
- Deller, A. T., Tingay, S. J., & Briske, W. 2009b, *ApJ*, 690, 198

- Deller, A. T., Verbiest, J. P. W., Tingay, S. J., & Bailes, M. 2008, *ApJ*, 685, L67
- De Luca, A., Caraveo, P. A., Esposito, P., & Hurley, K. 2009, *ApJ*, 692, 158
- Duncan, R. C., & Thompson, C. 1992, *ApJ*, 392, L9
- Fuchs, Y., Mirabel, F., Chaty, S., Claret, A., Cesarsky, C. J., & Cesarsky, D. A. 1999, *A&A*, 350, 891
- Halpern, J. P., & Gotthelf, E. V. 2010, *ApJ*, 725, 1384
- Helfand, D. J., Chatterjee, S., Briske, W. F., Camilo, F., Reynolds, J., van Kerkwijk, M. H., Halpern, J. P., & Ransom, S. M. 2007, *ApJ*, 662, 1198
- Hobbs, G., Lorimer, D. R., Lyne, A. G., & Kramer, M. 2005, *MNRAS*, 360, 974
- Gaensler, B. M., Slane, P. O., Gotthelf, E. V., & Vasisht, G. 2001, *ApJ*, 559, 963
- Gelfand, J. D., & Gaensler, B. M. 2007, *ApJ*, 667, 1111
- Kaplan, D. L., Chatterjee, S., Hales, C. A., Gaensler, B. M., & Slane P. O. 2009, *AJ*, 137, 354
- Kasen, D., & Bildsten, L. 2010, *ApJ*, 717, 245
- Kettenis, M., van Langevelde, H. J., Reynolds, C., & Cotton, B. 2006, in *ASP Conf. Ser.*, Vol. 351, *Astronomical Data Analysis Software and Systems XV*, ed. C. Gabriel, C. Arviset, D. Ponz, & S. Enrique, 497
- Levin, L., et al. 2010, *ApJ*, 721, L33
- MacMillan, D. S., & Ma, C. 2007, *Journal of Geodesy*, 81, 443
- Petrov, L., Phillips, C., Bertarini, A., Murphy, T., & Sadler, E. M. 2011, *MNRAS*, 414, 2528
- Pradel, N., Charlot, P., & Lestrade, J.-F. 2006, *A&A*, 452, 1099
- Tiengo, A., et al. 2010, *ApJ*, 710, 227
- Thompson, C., & Duncan, R. C. 1993, *ApJ*, 408, 194
- Vink, J., & Kuiper, L. 2006, *MNRAS*, 370, L14
- Vrba, F. J., Henden, A. A., Luginbuhl, C. B., Guetter, H. H., Hartmann, D. H., & Klose, S. 2000, *ApJ*, 533, L17

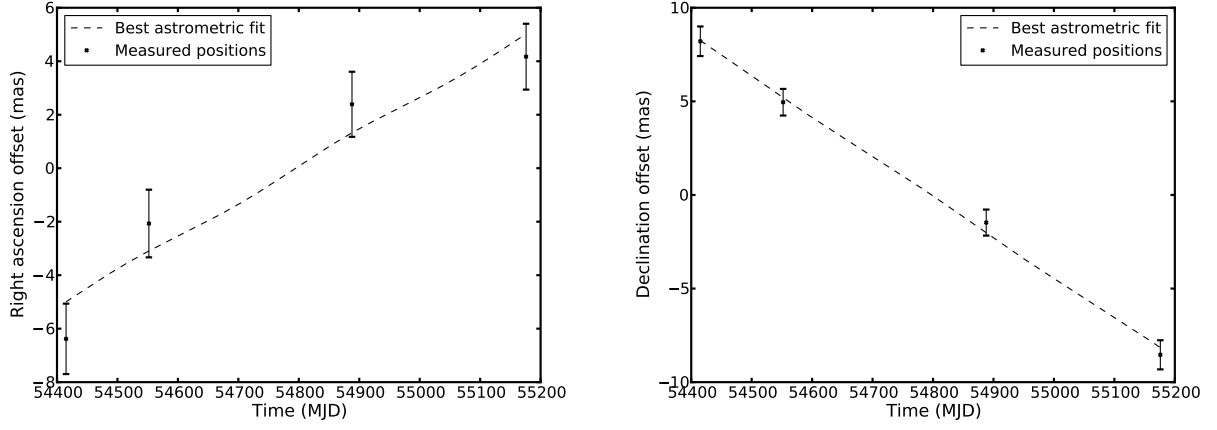


Fig. 1.— Motion of PSR J1550–5418, with measured positions overlaid on the best fit, and shown as offsets from the best-fit position at MJD 54795.0 (Table 2). **(Left)** Motion in Right Ascension vs time. **(Right)** Motion in declination vs time.